

Identification of Empty Land Based on Google Earth Using Convolutional Neural Network Algorithm

Islam Nur Alam^{*1}, Renaldy Fredyan², Ghinaa Zain Nabiilah³, Samsul Arifin⁴

Submitted: 09/11/2022 Accepted: 10/02/2023

Abstract: The development of digital image technology has experienced rapid development, both in terms of the development of models and algorithms used as well as the quality and results of the management process carried out. Utilization of digital image management can be used in classifying the condition of vacant land in certain areas. A high level of urbanization causes an increase in population growth and uneven development in certain areas. Advanced technology has resulted in a vast constellation of satellites and aerial platforms. In general, many remote sensing images with an excellent spatial resolution (VFSR) are commercially available to the general public, like google earth. This platform provides much information regarding spatial conditions. So, data available on the platform allows it to be used as a medium for analyzing and classifying the availability of vacant land in certain areas. To support good regional and city planning and overcome problems due to high levels of urbanization, a model that can automatically classify vacant land in certain areas is needed using data that is openly available on Google Earth. Thus, this study experimented by classifying vacant land based on images from google earth using the Deep Learning model, namely Convolutional Neural Network (CNN). The CNN method is used because of its superiority in classifying images. The experiment results have an optimal for image classification using the CNN algorithm.

Keywords: CNN, Google Earth, Vacant Land Classification

1. Introduction

Urban and regional planning is a complicated problem since many people live in their area based on their characteristics. Land Use and Land Cover (LULC) information is important to monitor and manage them properly to collect the real conditions in the geospatial field [1]. In addition, other problems such as food diffidence, disaster risk, and also poverty can be handled using Land Use and Land Cover information [2]. In general, a large number of remote sensing images with very fine spatial resolution (VFSR) are commercially available to the general public thanks to advancements in remote sensing technology, with Google Earth serving as the most useful example in this regard. This platform provides a lot of information regarding spatial conditions. In addition, VFSR can provide an opportunity for one to capture and study fine-grained LULC specifications, but due to limited information it cannot be interpreted efficiently. Significant work has been done in recent decades to automate the LULC classification method using VFSR images [3]. If you look at the existing methods, they can be categorized into several types, such as pixel-based and object-based approaches, which are currently developing quite rapidly. The pixel-based method currently under development has the specific goal of classifying individual pixels to process data based on spatial reflectance, but offered the spatial and spectral complexity involved in VFSR remote sensing images, this frequently results in a spectral noise effect with limited classification accuracy and thus becomes an

annoyance.

Using kernels or moving windows, contextual information can be combined to create spatial pattern characters [4]. This method is based on images that are randomly formed, whereas real items are frequently irregularly shaped and organized in predetermined patterns [5]. Since segmented objects (pixel groups) can be used to identify elements inside objects (spectra, texture, shape, etc.) and context between neighboring sections, object-based approaches are now frequently employed to categorize LULC images. Extracting information is possible. The choice of an appropriate segmentation scale to generate meaningful objects (such as particular categories of land cover), sub-segmentation, and top-segmentation within a single image will occur, which is a difficulty for such object-based techniques [6]. In order for the classifier to produce equivalent results when applied to various datasets, the extracted features that characterize the objects are also hand-coded through feature engineering, according to each user's knowledge and expertise is challenging [7]. Additionally, it can be exceedingly challenging to encode the spatial organization of land-use items into explicit attributes, which restricts their ability to be represented and distinguished using conventional techniques. Furthermore, LULC classes are frequently employed interchangeably in the categorization of remote sensing imagery [8], and traditional approaches do not explicitly identify the classification hierarchy (i.e., the degree of landscape representation). Land usage (LU) and land cover (LC), however, are ontologically represented at separate levels. Low-level status is denoted by LC, and high-level landscape characteristics are denoted by LU [9].

There are two fundamental issues with the current LULC classification algorithms (using conventional techniques and deep learning). (1) Classification Hierarchy Definition. (2) Establish the ideal scale for displaying the landscape. Land usage (LU) and land cover (LC) are frequently used interchangeably in taxonomic

1,2,3 Computer Science Department, BINUS Graduate Program - Master of Computer Science, Bina Nusantara University, Jakarta, 11480, Indonesia

ORCID ID : 0000-0001-5320-5534

4 Statistics Department, School of Computer Science, Bina Nusantara University, Jakarta, 11480, Indonesia

ORCID ID : 0000-0003-0805-0582

* Corresponding Author Email: islam.alam@binus.ac.id

hierarchies without accounting for their fundamentally different semantic meanings. The Earth's surface is described by LC, which is a mosaic of many LC categories, whereas LU is referred to as a high-level function in a particular space.

In terms of scale selection, it is challenging to identify the best size that can accurately capture the entirety of complex and heterogeneous landscapes; therefore, multi-scale feature representations are used to capture both large and tiny land features at different scales. frequently is A number of these scales have been thoroughly investigated by trial and error and tested through considerable experimentation with many possible scale combinations [10]. However, parameterizing such scales requires substantial CNN model training and takes a lot of time for deep learning approaches (like CNN). Additionally, deep pixels are available on the Google Earth platform to create surface forms. This might be a novel approach to employing a better CNN to pinpoint his LULC.

2. Related Works

Deep learning has enabled computer vision and pattern recognition to grow quickly in recent years, improving the accuracy of learning the most representative aspects of object hierarchies [11]. Convolutional neural networks (CNNs), a well-liked deep learning technique, have made significant advances in image processing and analysis [12]. It has impressively outperformed his abilities in a number of areas, not only in traditional computer vision fields like visual recognition, target recognition, and robotics, but also in many other real-world applications [12]. Through the use of high-level feature representation, CNN has demonstrated significant promise in a range of remote sensing applications, including road extraction. In the remote sensing domain, CNN has shown great potential in a wide variety of tasks through high-level feature representation, such as road extraction [13], vehicle detection [14], scene classification [15], semantic segmentation [16], and LULC image classification [17]. Through a hierarchy of filters, CNN networks analyse and extract high-level information from individual picture patches using a patch-based architecture. The magnitude of representations that appear throughout the landscape and, as a result, the classification accuracy of remote sensing images are significantly influenced by the choice of field size as a crucial CNN parameter. This scale also makes use of the vaguely defined LULC taxonomy structure. The remote sensing community is still grappling with the issue of determining the CNN scale for a certain LULC classification operation. Consider scale variety, or don't restrict the representation to a single scale, as a popular strategy [18]. Multiple scales have been incorporated into CNN networks in earlier studies to enhance the representation of spatial information at various scales [19]. For instance, numerous CNNs have been implemented with various patch sizes and dimensions. to increase the accuracy of scene classification, Deng et al. [20] improved feature representations at various scales. Multi-scale CNNs were utilized by Yang et al. to recognize complex scenes (airports, homes, businesses, etc.) in remote sensing photos with greater accuracy than single-scale CNN networks. The accuracy of target detection was increased by CNN's addition of finely defined characteristics at various scales and remote sensing identification of vehicles (ships, autos, etc.) in the picture [21]. Lv et al. [22] try to build of combining region-based multiscale CNNs for land cover item identification in remote sensing images achieves great efficiency and accuracy. Additionally, a their CNN built on objects and using two different sizes was created to

handle challenging land-use classification task [23]. In order to increase the precision of land cover categorization of hyperspectral data, deep features at different sizes were retrieved via a CNN network [24]. The difficulty of this multiscale CNN method, however, is figuring out the best scaling (patch size) for a big sample space, which is very challenging to examine in depth over the entire scale range.

In order to effectively and efficiently handle the scale issue when classifying remote sensing photos using Google Earth, this work was designed to represent the layered relationship between LU and LC. CNN networks used to be derived autonomously as sequence representations, so our goal is to provide an automated method that can be used in practice. The rest of this essay is organized as follows: the proposed method, followed by an analysis of results and discussion, and the last one is the conclusion.

3. Convolutional Neural Network

One of Deep Learning method that most of researcher use is Convolutional Neural Network (CNN). Because it is very useful, especially when used to find patterns in an image and then recognize objects in the image. Hubel and Wiesel first conducted the initial research that underlies the discovery of CNN regarding the visual cortex of the cat's sense of sight [4]. Image classification using MLP can already be done, but when it is used to classify large amounts of data, the accuracy it gets decreases. Therefore, the CNN algorithm was developed because it can directly study the data contained in the image and then use the pattern obtained to classify it.

There have been many studies on this CNN, resulting in new models that have been recognized worldwide, such as AlexNet [5], Le-Net5 [6], VGG16 [7] and many other models formed from this method. This algorithm is very good for identifying or recognizing objects with a large amount of data.

Convolutional Neural Network Algorithm is an algorithm that consists of several layers with a 3D arrangement (height, width and depth). The height and width are the pixel sizes of the image to be identified, while the depth is the number of layers in the image. In terms of age, the architecture of the CNN algorithm is divided into 2 main parts, namely [8]:

- Feature Learning, this section is the part where the image to be identified is first extracted to get the features stored in the image. This section is located at the front and consists of several interconnected layers that function to perform an extraction. The convolution layer is the first layer, and the pooling layer is the second. There is an activation layer for each layer that turns on the functions there.
- Classification, this section is the second part that functions to classify the images trained in the feature learning section. It consists of several layers composed of neurons. This layer gets the previous layer's output in the form of a 1-D vector image.

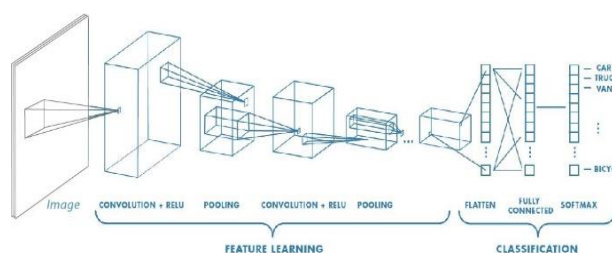


Fig. 1. CNN Architecture in General

Based on Fig. 1, the appropriate description for the layers is as follows:

1. Convolution Layer

The convolution layer is the first process that must be passed in the feature learning stage. In the convolution layer, a convolution operation will be performed between the input matrix and the kernel in the filter matrix. Convolution is a multiplication operation between two matrices which are then added together [16]. The result of the convolution process in the CNN algorithm is called a feature map. As input, the depth of an image is defined by the number of channels of the image. For example, if the image is 32x32x3, the number 3, which represents the number of layers in the image, can also measure the image's depth. In the convolution process, several parameters must be considered.

Table 1. Parameters of convolution layer

NO	Parameter	Description
1	Depth	Layer depth, be it an image layer or a feature layer
2	Stride	Number of shifts during convolution
3	Padding	The number of additions to zero values in the outer region of the image

Meanwhile, to calculate the number of convoluted feature maps can be calculated using the following formula:

$$\text{Output} = (W - N + 2P) / S + 1 \quad (1)$$

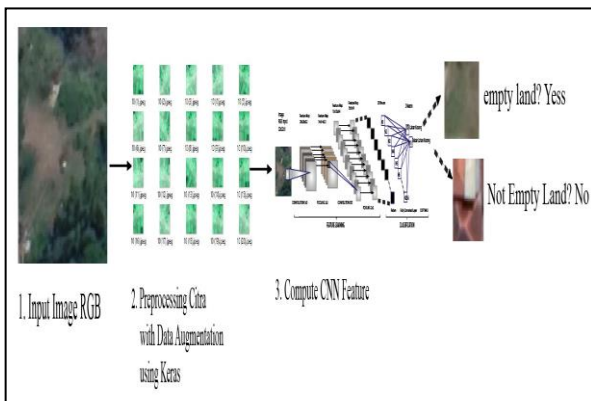


Fig. 2. Multi-Layer Neural Network

2. Image Preprocessing with Data Augmentation using KERAS Library.

- W = input length/height
- N = filter length/height
- P = padding
- S = stride

2. Pooling Layer

The pooling layer stage is situated following the convolution layer stage, as seen in the CNN architecture at the beginning of the discussion. A kernel of a specific size makes up this pooling layer, which will be applied with specific steps to the feature map produced by the convolution layer. There are two

popular pooling techniques; the first is average pooling, where the value taken is the average value of the matrix being pooled. The highest value should be used for the second max pooling.

3. Activation Layer

The Activation Layer determines whether the neuron must be "active" or not based on the input's weighted sum (weight of the sum). There are 2 types of activation functions in general: linear and non-linear.

Several kinds of activation functions that are often used in research include the sigmoid function, tanh, Rectified Linear Unit (ReLU), Leaky ReLU and Parametric ReLU [22].

4. Fully Connected Layer

The fully connected layer is a layer where all the neurons from the previous layers are combined into one for the classification process using a neural network. This layer is the same as the normal neural network layer; it can be in the form of a single net or MLP. However, before the classification process is carried out, the feature map generated from feature learning is still a multi-dimensional array, so it is necessary to convert it into vector form; this technique is called flattening. Flatten is a technique to reshape a feature map into a vector so that it can be used as input from a fully connected layer. So the input from the fully connected layer consists of one neuron resulting from reshaping the feature map into a vector. After flattening, all the weights will be classified according to the number of classes. However, several previous studies showed that using the MLP network could improve classification accuracy even though the difference was not very significant.

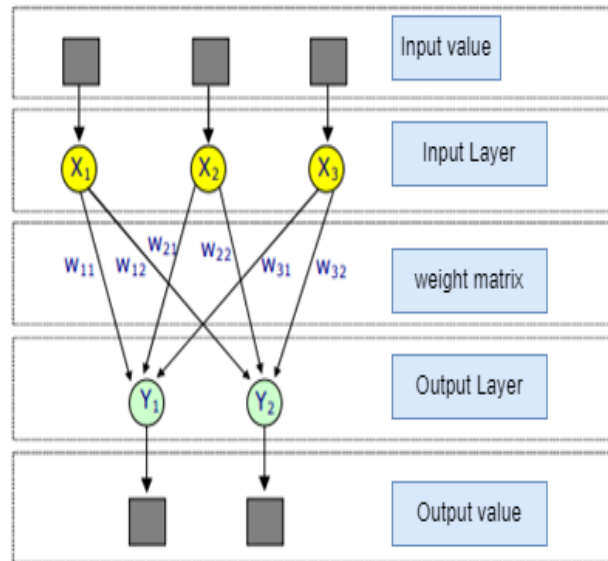


Fig. 3. System Design and Implementation

4. Method

In conducting this research, the first step was to collect a dataset containing photos from the cropped image of Google Earth, which was then divided into 2 parts, namely for data training and data testing. Before the data uses the CNN algorithm, the data will be preprocessed, namely cropping, RGB and data augmentation. After that, just do the architectural design of CNN. Starting with determining the depth of the layer, arranging the layers, and adding some regularization to improve the computational process. The following is a scenario and process design for the testing and training process in Fig 5.

4.1. System Design and Implementation

Before this research system is built, it is necessary to have a system design to be built first. The design of this system will be a big picture of how the system will be built later. From the system design, it will be seen where the CNN algorithm will be implemented. In simple terms, the design of the vacant land identification system based on google earth images can be seen in Fig 3.

4.1.1. Dataset Collection

In this study, an object in the form of a vacant land image needs to be identified to identify vacant land. Therefore, the data used is a cropped image of Google Earth. Moreover, the images identified in the study are 2 lands, namely, vacant land and not vacant land; previously, researchers carried out a survey of vacant land in Batu city.

4.1.2. Image Pre-processing

In this research, before the image is used as input for training, the image is processed first to make it easier for the CNN algorithm to conduct training and find the characteristics of the entered image. There are 2 stages of image pre-processing carried out before the image is processed by the CNN algorithm:



Fig. 4. Cropping Image

1. Image Cropping is done on the Google Earth Image in Fig 4.
2. Data Augmentation, expanding the number of images by manipulating the image without losing the core of the image in Fig 3.

4.1.3. Image Pre-processing

This study's architecture of the CNN algorithm consists of a 6-layer depth, as shown in Fig 6. From the architecture above, a regularization method, namely Dropout, is added. Giving Dropout aims to reduce the number of parameters that are not trained during computation. Added Dropouts are placed after Pooling Layer 2 and the first Layer on the FC Layer.

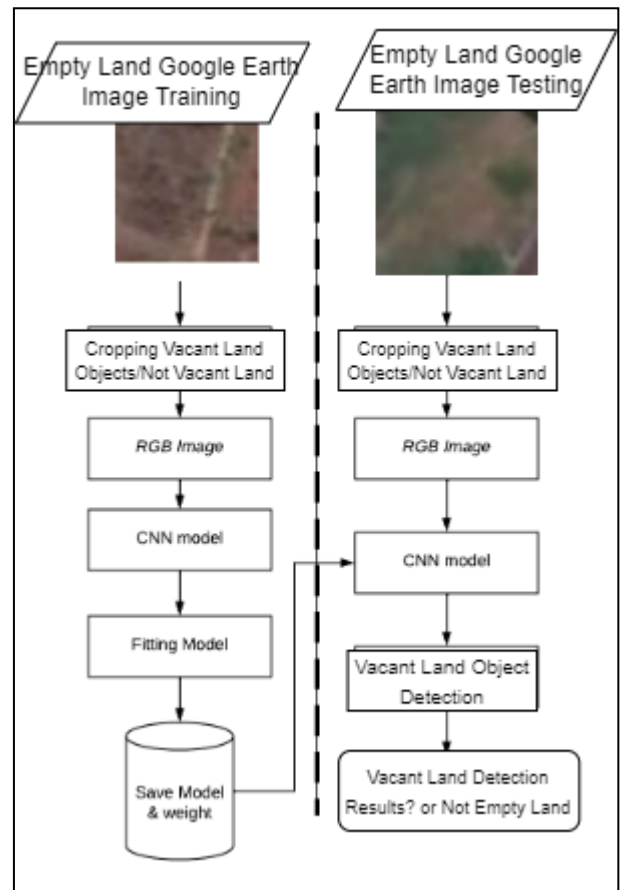


Fig. 5. Training and Testing Scenario

5. Experimental Results

5.1. Training Result

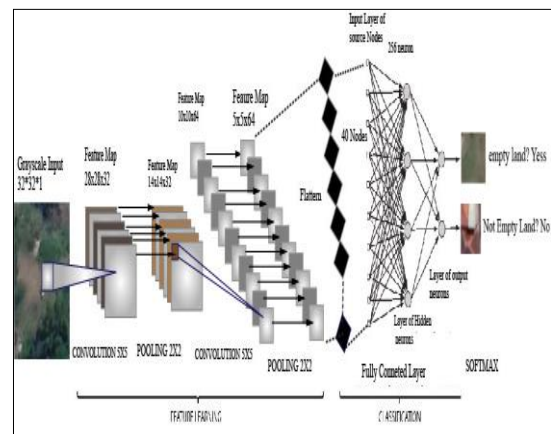


Fig. 6. CNN Architectural Design

One of the most critical parts of successfully identifying Batu city's vacant land based on Google Earth imagery is the excellent result of this training process. In this training process, 1000 images will be trained. The iteration parameter carried out in this training process is 1000 epochs with a batch size value of 16. So the training process will be repeated 1000 times to obtain feature extraction from the required features. Then the learning rate value used in this training process is 0.001. This learning rate value is used to update the weights each time the algorithm performs a backwards-pass process. Finally, calculating accuracy is done by entering the prediction results in the table as in Table 2.

Table 2. Confussion Matrix of Training Result

Matriks		Predict Class	
		Empty Land	Not Empty Land
Actual Class	Empty Land	517	3
	Not Empty Land	2	478

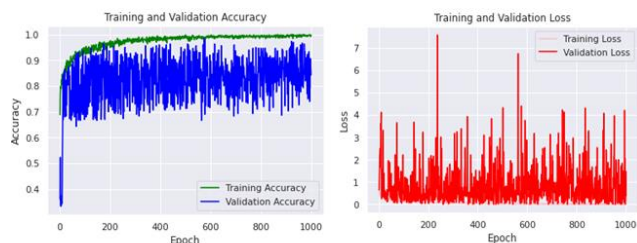


Fig. 7. Graph of accuracy and loss value

From Table 2 above, it can be seen that the accuracy of the training process is 99.5%. Furthermore, this accuracy value can be expressed on a graph of the training process results after running 1000 epochs using a tensorboard.

5.2. Testing Result

The model from the training results that have been stored is then recalled to carry out the testing process in this testing process uses test data as many as 300 images, which are divided into 2 classes. So each class of prediction types consists of 100 empty land images and 200 non-vacant land images. The results of this test are then entered into a more concise prediction table in Table 3.

Table 3. Confussion Matrix of Testing Result

Matriks		Predict Class	
		Empty Land	Not Empty Land
Actual Class	Empty Land	82	23
	Not Empty Land	18	177

Based on the table of prediction results above, the prediction results from the model to the testing data show good results. For example, in the vacant land class of 100 data tested, there are only 18 data that have wrong predictions. While in the non-vacant land class of 200 data, there are 23 incorrect data from the table, the accuracy can be calculated as follows:

$$Accuracy = \frac{\text{All True Positive}}{\text{Total Number Testing}} \times 100\% \quad (2)$$

$$Accuracy = \frac{259}{300} \times 100\% = 86.34\% \quad (3)$$

From these calculations, the accuracy of the identification of vacant land based on google earth images using the CNN algorithm is 86.34%. The results obtained from the calculation of accuracy using the confusion matrix were lower than the calculation using the method. The effect of the number of epochs is shown in table 4.

Table 4. The effect of the number of epochs

Epocs	Accuracy	Loss value	Time
500	83.67%	0.41	29 minutes
1000	80.59%	0.76	41minutes

1500	85.25%	0.16	1 hour 6 minutes
------	--------	------	------------------

Table 5. The effect of the number of learning rate

Learning rate	Akurasi	Loss value	Time
0.01	74.54%	3.46	1 hour 5 minutes
0.001	95.63%	0.07	1 hour 2 minutes
0.0001	81.65%	0.16	59 minutes

Table 6. Image Size Effect

Image Size	Accuracy	Loss value	Time
32x32	95.63%	0.07	1 hour 5 minutes
64x64	84.24%	1.42	1 hour 15 minutes
128x128	86.98%	0.01	2 hour 3 minutes

6. Conclusions

From the results of research carried out to identify vacant land in Batu City based on google earth images using the Convolutional Neural Network (CNN) method, it can be concluded that the CNN algorithm is quite good in identifying vacant land based on Google Earth images. Training at 1000 epochs and a learning rate of 0.001 means the training accuracy is 99.5%, and the testing accuracy is 86.34%. This result is quite good considering the quality and amount of data obtained are not so good, and the amount is not much. In addition, the limited capabilities of the device are also quite influential on the results of this study. Due to the devices' limitations, it is difficult for researchers to experiment with more complex layer arrangements.

References

- [1] B. Zhao, Y. Zhong, and L. Zhang, "A spectral-structural bag-of-features scene classifier for very high spatial resolution remote sensing imagery," *ISPRS J. Photogramm. Remote Sens.*, vol. 116, pp. 73–85, 2016, doi: <https://doi.org/10.1016/j.isprsjprs.2016.03.004>.
- [2] J. Stürck, C. J. E. Schulp, and P. H. Verburg, "Spatio-temporal dynamics of regulating ecosystem services in Europe – The role of past and future land use change," *Appl. Geogr.*, vol. 63, pp. 121–135, 2015, doi: <https://doi.org/10.1016/j.apgeog.2015.06.009>.
- [3] C. Zhang *et al.*, "Joint Deep Learning for land cover and land use classification," *Remote Sens. Environ.*, vol. 221, pp. 173–187, 2019, doi: <https://doi.org/10.1016/j.rse.2018.11.014>.
- [4] F. Melgani and S. B. Serpico, "A statistical approach to the fusion of spectral and spatio-temporal contextual information for the classification of remote-sensing images," *Pattern Recognit. Lett.*, vol. 23, no. 9, pp. 1053–1061, 2002, doi: [https://doi.org/10.1016/S0167-8655\(02\)00052-1](https://doi.org/10.1016/S0167-8655(02)00052-1).
- [5] C. Zhang, P. A. Harrison, X. Pan, H. Li, I. Sargent, and P. M. Atkinson, "Scale Sequence Joint Deep Learning (SS-JDL) for land use and land cover classification," *Remote Sens. Environ.*, vol. 237, no. September 2019, p. 111593, 2020, doi: [10.1016/j.rse.2019.111593](https://doi.org/10.1016/j.rse.2019.111593).
- [6] D. Ming, J. Li, J. Wang, and M. Zhang, "Scale parameter selection by spatial statistics for GeOBIA: Using mean-shift based multi-scale segmentation as an example," *ISPRS J. Photogramm. Remote Sens.*, vol. 106, pp. 28–41, 2015, doi: <https://doi.org/10.1016/j.isprsjprs.2015.04.010>.
- [7] Y. Yao *et al.*, "Classifying land-use patterns by integrating time-series electricity data and high-spatial resolution remote sensing imagery," *Int. J. Appl. Earth Obs. Geoinf.*, vol. 106, p. 102664, 2022, doi: <https://doi.org/10.1016/j.isprsjprs.2015.04.010>.

- <https://doi.org/10.1016/j.jag.2021.102664>.
- [8] J. Jin *et al.*, “Heterogeneity of land cover data with discrete classes obscured remotely-sensed detection of sensitivity of forest photosynthesis to climate,” *Int. J. Appl. Earth Obs. Geoinf.*, vol. 104, p. 102567, 2021, doi: <https://doi.org/10.1016/j.jag.2021.102567>.
- [9] X. Cheng *et al.*, “Enhanced contextual representation with deep neural networks for land cover classification based on remote sensing images,” *Int. J. Appl. Earth Obs. Geoinf.*, vol. 107, p. 102706, 2022, doi: <https://doi.org/10.1016/j.jag.2022.102706>.
- [10] M. Kim, T. A. Warner, M. Madden, and D. S. Atkinson, “Multi-scale GEOBIA with very high spatial resolution digital aerial imagery: scale, texture and image objects,” *Int. J. Remote Sens.*, vol. 32, no. 10, pp. 2825–2850, May 2011, doi: 10.1080/01431161003745608.
- [11] Y. Wang, B. Xiao, A. Bouferguene, M. Al-Hussein, and H. Li, “Vision-based method for semantic information extraction in construction by integrating deep learning object detection and image captioning,” *Adv. Eng. Informatics*, vol. 53, p. 101699, 2022, doi: <https://doi.org/10.1016/j.aei.2022.101699>.
- [12] E. Paul and S. R.S., “Modified convolutional neural network with pseudo-CNN for removing nonlinear noise in digital images,” *Displays*, vol. 74, p. 102258, 2022, doi: <https://doi.org/10.1016/j.displa.2022.102258>.
- [13] G. Cheng, Y. Wang, S. Xu, H. Wang, S. Xiang, and C. Pan, “Automatic Road Detection and Centerline Extraction via Cascaded End-to-End Convolutional Neural Network,” *IEEE Trans. Geosci. Remote Sens.*, vol. 55, no. 6, pp. 3322–3337, 2017, doi: 10.1109/TGRS.2017.2669341.
- [14] Y. Dong, L. Zhang, L. Zhang, and B. Du, “Maximum margin metric learning based target detection for hyperspectral images,” *ISPRS J. Photogramm. Remote Sens.*, vol. 108, pp. 138–150, 2015, doi: <https://doi.org/10.1016/j.isprsjprs.2015.07.003>.
- [15] X. Liu *et al.*, “Classifying urban land use by integrating remote sensing and social media data,” *Int. J. Geogr. Inf. Sci.*, vol. 31, no. 8, pp. 1675–1696, Aug. 2017, doi: 10.1080/13658816.2017.1324976.
- [16] H. Wang, Y. Wang, Q. Zhang, S. Xiang, and C. Pan, “Gated Convolutional Neural Network for Semantic Segmentation in High-Resolution Images,” *Remote Sensing*, vol. 9, no. 5, 2017. doi: 10.3390/rs9050446.
- [17] C. Zhang *et al.*, “A hybrid MLP-CNN classifier for very fine resolution remotely sensed image classification,” *ISPRS J. Photogramm. Remote Sens.*, vol. 140, pp. 133–144, 2018, doi: <https://doi.org/10.1016/j.isprsjprs.2017.07.014>.
- [18] X. Pan and J. Zhao, “High-Resolution Remote Sensing Image Classification Method Based on Convolutional Neural Network and Restricted Conditional Random Field,” *Remote Sensing*, vol. 10, no. 6, 2018. doi: 10.3390/rs10060920.
- [19] Z. Yang, X. Mu, and F. Zhao, “Scene classification of remote sensing image based on deep network and multi-scale features fusion,” *Optik (Stuttg.)*, vol. 171, pp. 287–293, 2018, doi: <https://doi.org/10.1016/j.ijleo.2018.06.024>.
- [20] Z. Deng, H. Sun, S. Zhou, J. Zhao, L. Lei, and H. Zou, “Multi-scale object detection in remote sensing imagery with convolutional neural networks,” *ISPRS J. Photogramm. Remote Sens.*, vol. 145, pp. 3–22, 2018, doi: <https://doi.org/10.1016/j.isprsjprs.2018.04.003>.
- [21] Q. Li, L. Mou, Q. Liu, Y. Wang, and X. X. Zhu, “HSF-Net: Multiscale Deep Feature Embedding for Ship Detection in Optical Remote Sensing Imagery,” *IEEE Trans. Geosci. Remote Sens.*, vol. 56, no. 12, pp. 7147–7161, 2018, doi: 10.1109/TGRS.2018.2848901.
- [22] X. Lv, D. Ming, T. Lu, K. Zhou, M. Wang, and H. Bao, “A New Method for Region-Based Majority Voting CNNs for Very High Resolution Image Classification,” *Remote Sensing*, vol. 10, no. 12, 2018. doi: 10.3390/rs10121946.
- [23] C. Zhang, I. Sargent, X. Pan, A. Gardiner, J. Hare, and P. M. Atkinson, “VPRS-Based Regional Decision Fusion of CNN and MRF Classifications for Very Fine Resolution Remotely Sensed Images,” *IEEE Trans. Geosci. Remote Sens.*, vol. 56, no. 8, pp. 4507–4521, 2018, doi: 10.1109/TGRS.2018.2822783.
- [24] N. He *et al.*, “Feature Extraction With Multiscale Covariance Maps for Hyperspectral Image Classification,” *IEEE Trans. Geosci. Remote Sens.*, vol. 57, no. 2, pp. 755–769, 2019, doi: 10.1109/TGRS.2018.2860464.